
Approximate inference of marginals using the IBIA framework

Shivani Bathla

Department of Electrical Engineering
IIT Madras
India, 600036
ee13s064@ee.iitm.ac.in

Vinita Vasudevan

Department of Electrical Engineering
IIT Madras
India, 600036
vinita@ee.iitm.ac.in

Abstract

Exact inference of marginals in probabilistic graphical models (PGM) is known to be intractable, necessitating the use of approximate methods. Most of the existing variational techniques perform iterative message passing in loopy graphs which is slow to converge for many benchmarks. In this paper, we propose a new algorithm for marginal inference that is based on the incremental build-infer-approximate (IBIA) paradigm. Our algorithm converts the PGM into a *sequence of linked clique tree forests (SLCTF)* with bounded clique sizes, and then uses a heuristic belief update algorithm to infer the marginals. For the special case of Bayesian networks, we show that if the incremental build step in IBIA uses the topological order of variables then (a) the prior marginals are consistent in all CTFs in the SLCTF and (b) the posterior marginals are consistent once all evidence variables are added to the SLCTF. In our approach, the belief propagation step is non-iterative and the accuracy-complexity trade-off is controlled using user-defined clique size bounds. Results for several benchmark sets from recent UAI competitions show that our method gives either better or comparable accuracy than existing variational and sampling based methods, with smaller runtimes.

1 Introduction

Discrete probabilistic graphical models (PGM) including Bayesian networks (BN) and Markov networks (MN) are used for probabilistic inference in a wide variety of applications. An important task in probabilistic reasoning is the computation of posterior marginals of all the variables in the network. Exact inference is known to be #P-complete [Roth, 1996], thus necessitating approximations. Approximate techniques can be broadly classified as sampling based and variational methods.

Sampling based methods include Markov chain Monte Carlo based techniques like Gibbs sampling [Gelfand, 2000, Kelly et al., 2019] and importance sampling based methods [Gogate and Dechter, 2011, Friedman and Van den Broeck, 2018]. An advantage of these methods is that accuracy can be improved with time without increasing the required memory. However, in many benchmarks the improvement becomes very slow with time. Alternatively, variational techniques can be used. These include loopy belief propagation (LBP) [Frey and MacKay, 1998, Wainwright et al., 2002], region-graph based techniques like generalized belief propagation (GBP) [Yedidia et al., 2000] and its variants [Heskes et al., 2003, Mooij and Kappen, 2007, Lin et al., 2020], mini-bucket based schemes like iterative join graph propagation (IJGP) [Mateescu et al., 2010] and weighted mini-bucket elimination (WMB) [Liu and Ihler, 2011] and methods that simplify the graph structure like edge deletion belief propagation (EDBP) and the related relax-compensate-recover (RCR) techniques [Choi et al., 2005, Choi and Darwiche, 2006, 2010]. While the accuracy-complexity trade-off can be achieved using a single user-defined clique size bound in mini-bucket based methods, it is non-trivial in many of the other region graph

based methods. Most of these techniques use iterative message passing to solve an optimization problem, for which convergence is not guaranteed and even if possible, can be slow to achieve.

The recently proposed *incremental build-infer-approximate* (IBIA) framework [Bathla and Vasudevan, 2023] uses a different approach. It converts the PGM into a sequence of calibrated clique tree forests (SCTF) with clique sizes bounded to a user-defined value. Bathla and Vasudevan [2023] show that the normalization constant (NC) of clique beliefs in the last CTF in the sequence is the estimate of the partition function of the overall distribution. This framework has two main advantages. Firstly, since it is based on clique trees and not loopy graphs, the belief propagation step is non-iterative. Therefore, it is fast and has no issues related to convergence. Secondly, it provides an easy control of the accuracy complexity trade-off using two user-defined parameters. However, the framework in Bathla and Vasudevan [2023] cannot be used to infer marginals. This is because only the clique beliefs in the last CTF account for all factors in the PGM. Beliefs in all other CTFs account for a subset of factors and thus, cannot be used for inference of marginals.

Contributions of this work: In this paper, we propose a method for marginal inference that uses the IBIA framework. We show that the approximation algorithm used in this framework preserves the within-clique beliefs. Based on this property, we modify the data structure generated by IBIA to add links between adjacent CTFs. We refer to the modified data structure as a *sequence of linked clique tree forests* (SLCTF). We propose a heuristic belief update algorithm that re-calibrates all CTFs in the sequence such that the updated beliefs account for all factors in the PGM. Results for several UAI benchmark sets show that our method gives either better or comparable accuracy when compared to the existing variational and sampling based methods, with competitive runtimes.

For the special case of BNs, we show that if the incremental build step in IBIA is performed in the topological order of variables then (a) the estimated partition function is guaranteed to be one if no evidence variables are present (b) the prior marginals of all variables are consistent across all CTFs in the sequence and (c) once all the evidence variables have been added to the SLCTF, the posterior marginals of variables in subsequent CTFs are consistent. Our results show that using the topological ordering for BNs leads to better estimates of partition function, prior marginals and posterior marginals in most benchmarks.

2 Background

2.1 Discrete Probabilistic Graphical Models

Let $\mathcal{X} = \{X_1, X_2, \dots, X_n\}$ be a set of random variables with associated domains $D = \{D_{X_1}, D_{X_2}, \dots, D_{X_n}\}$. The probabilistic graphical model (PGM) over \mathcal{X} consists of a set of factors, Φ , where each factor $\phi_\alpha(\mathcal{X}_\alpha) \in \Phi$ is defined over a subset of variables, $Scope(\phi) = \mathcal{X}_\alpha$. Let D_α denote the Cartesian product of the domains of variables in \mathcal{X}_α , then $\phi_\alpha : D_\alpha \rightarrow R \geq 0$. The joint probability distribution captured by the PGM is $P(\mathcal{X}) = \frac{1}{Z} \prod_\alpha \phi_\alpha$, where $Z = \sum_{\mathcal{X}} \prod_\alpha \phi_\alpha$ is the partition function. PGMs can be broadly classified as Markov networks (MN) which are the undirected models and Bayesian networks (BN) which are the directed models.

One method to perform exact inference involves converting the PGM into a *clique tree* (CT), which is a hypertree where each node C_i is a clique that contains a subset of variables. We use the term C_i as a label for the clique as well as to denote the set of variables in the clique. An edge between C_i and C_j is associated with a set of *sepset variables* denoted $S_{i,j} = C_i \cap C_j$. Exact inference in a CT is done using the belief propagation (BP) algorithm [Lauritzen and Spiegelhalter, 1988] that is equivalent to two rounds of message passing along the edges of the CT. The algorithm returns a CT with calibrated clique beliefs $\beta(C_i)$ and sepset beliefs $\mu(S_{i,j})$. In a calibrated CT, all clique beliefs have the same normalization constant (Z) and beliefs of all adjacent cliques agree over the marginals of the sepset variables. The joint probability distribution, $P(\mathcal{X})$, can be rewritten as follows.

$$P(\mathcal{X}) = \frac{1}{Z} \frac{\prod_{i \in \mathcal{V}_T} \beta(C_i)}{\prod_{(i,j) \in \mathcal{E}_T} \mu(S_{i,j})} \quad (1)$$

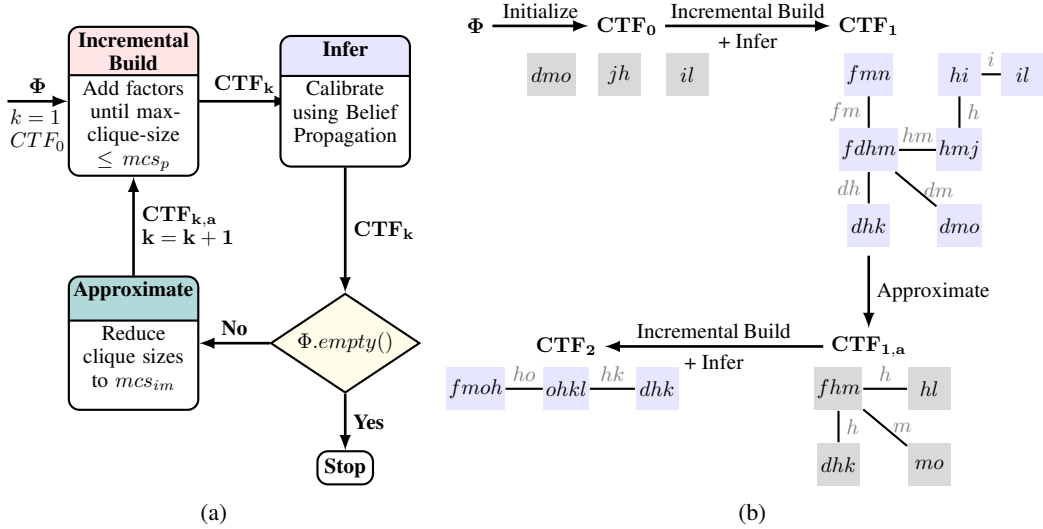


Figure 1: Conversion of the PGM, Φ , into a sequence of calibrated CTFs (SCTF) using the IBIA framework. (a) Overall methodology. (b) Construction of $SCTF = \{CTF_1, CTF_2\}$ for a PGM, $\Phi = \{\phi(d, m, o), \phi(j, h), \phi(i, l), \phi(f, m, n), \phi(h, i), \phi(d, h, k), \phi(f, d, h), \phi(j, m), \phi(k, l, o), \phi(f, o)\}$, with mcs_p and mcs_{im} set to 4 and 3 respectively. CTF_0 is formed using cliques corresponding to factors $\phi(d, m, o), \phi(j, h), \phi(i, l)$. CTF_1 contains all factors except $\phi(k, l, o), \phi(f, o)$. These factors are added to CTF_2 .

where \mathcal{V}_T and \mathcal{E}_T are the set of nodes and edges in the CT. The marginal probability distribution of a variable v can be obtained by marginalizing the belief of any clique C that contains v as follows.

$$P(v) = \frac{1}{Z} \sum_{C \ni v} \beta(C) \quad (2)$$

We use the following definitions in this paper.

Definition 1. Clique Tree Forest (CTF): Set of disjoint clique trees.

Definition 2. Clique size: The clique size cs of a clique C is the effective number of binary variables contained in C . It is computed as follows.

$$cs = \log_2 \left(\prod_{\forall v_i \in C} |D_i| \right) \quad (3)$$

where $|D_i|$ is the cardinality or the number of states in the domain of the variable v_i .

Definition 3. Prior marginals ($P(X_i)$): It is the marginal probability of a variable X_i when the PGM has no evidence variables.

Definition 4. Posterior marginals ($P(X_i|E = e)$): It is the conditional probability distribution of a variable X_i , given a fixed evidence state e .

2.2 Overview of IBIA framework

Methodology: The IBIA framework proposed in Bathla and Vasudevan [2023] converts the PGM into a sequence of calibrated CTFs (SCTF) with bounded clique sizes. IBIA starts with an initial CTF, CTF_0 , that contains cliques corresponding to factors with disjoint scope. Figure 1a illustrates the overall methodology used in the framework. It uses three main steps as described below.

Incremental Build: In this step, a CTF, CTF_k , is constructed by incrementally adding factors in the PGM to an initial CTF (CTF_0 or $CTF_{k-1,a}$) until the maximum clique size reaches a user-specified bound mcs_p . Methods for incremental construction of CTs have been proposed in Bathla and Vasudevan [2023] and Flores et al. [2002]. Either of the two methods can be used to incrementally add new factors.

Infer: In this step, all CTs in CTF_k are calibrated using the standard belief propagation algorithm.

Approximate: In this step, CTF_k is approximated to give an approximate CTF, $CTF_{k,a}$, that has clique sizes reduced to another user-specified bound mcs_{im} .

As shown in Figure 1a, IBIA constructs the $SCTF = \{CTF_1, \dots, CTF_n\}$ by repeatedly using the incremental build, infer and approximate steps. This process continues until all factors in the PGM are added to some CTF in the SCTF. Figure 1b shows the SCTF generated by IBIA for an example PGM, Φ (specified in the caption to the figure), with clique size bounds mcs_p and mcs_{im} set to 4 and 3 respectively. For the purpose of illustrating all steps, the disjoint cliques corresponding to factors $\phi(d, m, o)$, $\phi(i, l)$ and $\phi(j, h)$ are chosen as the initial CTF, CTF_0 . CTF_1 is constructed by incrementally adding factors to CTF_0 . All factors except $\phi(k, l, o)$ and $\phi(f, o)$ are added to CTF_1 . These two factors are deferred since their addition results in clique sizes greater than $mcs_p = 4$. CTF_1 is calibrated using BP and then approximated to give $CTF_{1,a}$ with clique sizes bounded to $mcs_{im} = 3$. CTF_2 is constructed by adding the remaining factors to $CTF_{1,a}$. We will use this example to explain the steps in our method for inference of marginals.

Approximate step: Since our inference algorithm is based on the properties of the approximate CTF, we explain this step in more detail using the running example shown in Figure 1b. Variables f, k, l and o in CTF_1 are also present in the deferred factors $\phi(k, l, o)$ and $\phi(f, o)$. These variables are needed for the construction of subsequent CTFs and are called *interface variables* (IV). All other variables in CTF_1 are called *non-interface variables* (NIV). $CTF_{1,a}$ is initialized as the minimal subgraph that connects the IVs. This subgraph contains all cliques in CTF_1 except clique fmn . Approximation involves two main steps to reduce the number of cliques and clique sizes.

1. *Exact marginalization*: The goal of this step is to remove as many NIVs as possible while ensuring that the overall joint distribution is preserved. NIV j is present in a single clique hmj and is marginalized out from it by summing over the states of j . The resulting clique hm is a non-maximal clique that is contained in clique $fdhm$, and is thus removed. NIV i is removed after collapsing containing cliques hi and il . Exact marginalization of the other NIVs results in collapsed cliques with size greater than $mcs_{im} = 3$, and is not performed.

2. *Local marginalization*: In this step, clique sizes are reduced by marginalizing variables from individual cliques with size greater than mcs_{im} while ensuring that (a) $CTF_{1,a}$ is a valid CTF that satisfies the running intersection property (RIP) (b) a connected CT in CTF_1 remains connected in $CTF_{1,a}$ and (c) $CTF_{1,a}$ contains all IVs. To reduce the size of the large-sized clique $fdhm$, NIV d is locally marginalized from this clique. In order to satisfy RIP, it needs to be marginalized from either clique dmo or dhk . Here, d is locally marginalized from clique dmo to give $CTF_{1,a}$ as shown in the figure. Since all cliques containing d are not collapsed before marginalization, this results in an approximate joint distribution.

Bathla and Vasudevan [2023] show that all CTs in the approximate CTF obtained after exact and local marginalization are valid and calibrated.

3 Inference of marginals

In this section, we first discuss some of the properties satisfied by the SCTF generated by IBIA. Based on these properties, we then describe the proposed methodology for inference of marginals.

3.1 Properties of SCTF

We show that each CTF_k in SCTF and the corresponding approximate CTF, $CTF_{k,a}$, satisfy the following properties. The detailed proofs for these properties are included in the supplementary material and the main ideas used in the proofs are discussed here.

Proposition 1. *The joint belief of variables contained within any clique in the approximate CTF $CTF_{k,a}$ is the same as that in CTF_k .*

Proof Sketch. Both exact and local marginalization involve summing clique beliefs over the states of a variable, which does not alter the joint belief of the remaining variables in the clique. \square

Proposition 2. *The clique beliefs in CTF_k account for all factors added to $\{CTF_1, \dots, CTF_k\}$.*

Proof Sketch. Using Proposition 5, the clique beliefs in $CTF_{1,a}$ are same as that in CTF_1 . CTF_2 is obtained after adding new factors to $CTF_{1,a}$. Therefore, after calibration, clique beliefs in CTF_2 account for factors added to CTF_1 and CTF_2 . The proposition follows, since the same argument holds true for all CTFs in the sequence. \square

BNs can be handled in a similar manner as MNs by using the undirected moralized graph corresponding to the BN. Another possibility is to use the directed acyclic graph (DAG) corresponding to the BN to guide the incremental build step. In contrast to MNs where all factors are un-normalized, each factor in a BN is the conditional probability distribution (CPD) of a variable y given the state of its parents in the DAG (Pa_y). Factors corresponding to the evidence variables are simplified based on the given state and hence become un-normalized. The following properties hold true if each CTF in the SCTF is built by adding factors in the topological order. By this, we mean that the factor corresponding to the variable y is added only after the factors corresponding to all parent variables in Pa_y have been added to some CTF in the sequence. Let Y_k denote the set of variable whose CPDs are added during construction of CTF_k , e_k denote the evidence states of all evidence variables in Y_k and Pa_{Y_k} denote the parents of variables in Y_k in the BN.

Proposition 3. *The product of factors added in CTFs, $\{CTF_1, \dots, CTF_k\}$ is a valid probability distribution whose normalization constant is the probability of evidence states e_1, \dots, e_k .*

Proof. For each variable $y \in \{Y_1, \dots, Y_k\}$, the corresponding CPD $P(y|Pa_y)$ is added to some CTF in $\{CTF_1, \dots, CTF_k\}$. The proposition follows since the CPDs corresponding to parents of y are always added to a CTF before the CPD of y is added. \square

Proposition 4. *The normalization constant of the distribution encoded by the calibrated beliefs in CTF_k is the estimate of probability of evidence states e_1, \dots, e_k .*

Proof Sketch. Using Proposition 3, the normalization constant (NC) of the distribution encoded by CTF_1 is $P(e_1)$. Using Proposition 5, the within-clique beliefs are preserved during approximation. This implies that the NC of $CTF_{1,a}$ is also $P(e_1)$. Although the NC is the same, the overall distribution corresponding to $CTF_{1,a}$ is approximate due to local marginalization. CTF_2 is constructed by adding CPDs of variables in Y_2 to $CTF_{1,a}$. CPDs of parent variables in Pa_{Y_2} are added either in CTF_1 or CTF_2 . Hence, after calibration, we get a valid probability distribution with NC as the estimate of probability of evidence states e_1, e_2 . A similar procedure can be used to show that the property holds for all CTFs. \square

Corollary 1. *For a BN with no evidence variables, the normalization constant of any CT in CTF_k is guaranteed to be one.*

Theorem 1. *Let I_E denote the index of the last CTF in the sequence where the factor corresponding to an evidence variable is added. The posterior marginals of variables present in CTFs $\{CTF_k, k \geq I_E\}$ are preserved and can be computed from any of these CTFs.*

Proof Sketch. Once all evidence variables are added, additional CPDs added in each new CTF in $\{CTF_k, k > I_E\}$ correspond to the successors in the BN. Since CPDs corresponding to all successors are normalized, the beliefs of the previous variables remain unchanged. \square

Corollary 2. *For a BN with no evidence variables, the estimate of prior marginals obtained from any CTF in the sequence is the same.*

3.2 Proposed algorithm for inference of marginals

We first explain our approach for estimation of marginals with the help of the example shown in Figure 1b. Following this, we formally describe the main steps in our algorithm.

The SCTF generated by IBIA for the example in Figure 1b contains two CTFs, CTF_1 and CTF_2 . Using Proposition 6, we know that calibrated clique beliefs in CTF_2 account for all factors in the PGM, Φ . Therefore, the marginals of all variables present in it can be inferred using Equation 2. However, clique beliefs in CTF_1 do not account for factors $\phi(k, l, o)$ and $\phi(f, o)$ which were added during the construction of CTF_2 . Therefore, in order to infer the marginals of variables n, j and i that are present only in CTF_1 , we need to update the beliefs to account for these two factors.

Figure 2 shows CTF_1 , $CTF_{1,a}$ and CTF_2 for the example. Using Proposition 5, we know that the joint belief of variables present within any clique in $CTF_{1,a}$ is the same as that in CTF_1 . However, this belief changes when new factors are added during the construction of CTF_2 . For instance, $\beta(C_2') = \sum_d \beta(C_2) \neq \sum_o \beta(\tilde{C}_2)$. To reflect the effect of new factors added in CTF_2 , the beliefs in C_2 can be updated as follows.

$$\beta(C_2) = \frac{\beta(C_2)}{\sum_d \beta(C_2)} \sum_o \beta(\tilde{C}_2)$$

To make sure that CTF_1 remains calibrated, this must be followed by a single round of message passing in CTF_1 with C_2 as the root node. It is clear that a similar belief update is needed for all the variables in $CTF_{1,a}$. However, every update and subsequent round of message passing will override the previous updates. Hence, the beliefs in CTF_1 will only approximately reflect the effect of additional factors in CTF_2 . To improve accuracy, we propose a heuristic procedure for belief update sequence.

Formally, the steps in our algorithm are as follows. Variables present in $CTF_{k,a}$ are present in both CTF_k and CTF_{k+1} . We refer to these variables as the *link variables*. We first find links between corresponding cliques $C \in CTF_k$, $C' \in CTF_{k,a}$ and $\tilde{C} \in CTF_{k+1}$. Each link (C, C', \tilde{C}) is associated with a set of link variables $V_l = C \cap C'$. For the example, links between CTF_1 , $CTF_{1,a}$ and CTF_2 , and the corresponding link variables are shown in magenta in Figure 2. The first part of a link contains cliques C' and C . It is obtained as follows.

(a) If C' is obtained after collapsing a set of cliques $\{C_1, \dots, C_m\}$ in CTF_k , C' is linked to each of $\{C_1, \dots, C_m\}$. For example, C_4' is linked to C_4 and C_5 , which were collapsed during exact marginalization of variable i .

(b) If C' is obtained from C in CTF_k after local marginalization, C' is linked to C . In the example, cliques C_1' and C_2' are obtained after local marginalization of variable d from cliques C_1 and C_2 respectively. Hence, the corresponding tuples are (C_1, C_1') and (C_2, C_2') .

(c) If C' is same as clique C in CTF_k , C' is linked to C . For example, C_3 is linked to C_3' .

The second part links C' to \tilde{C} in CTF_{k+1} such that $C' \subseteq \tilde{C}$. This is always possible since CTF_{k+1} is obtained after incrementally modifying $CTF_{k,a}$ to add new factors. Thus, each clique in $CTF_{k,a}$ is contained in some clique in CTF_{k+1} . For example, $C_1' \subseteq \tilde{C}_2$ and the link is (C_1, C_1', \tilde{C}_2) .

We refer to the modified data structure consisting of the sequence of calibrated CTFs, $SCTF = \{CTF_k\}$ and a list of links between all adjacent CTFs, $SL = \{L_k\}$, as the *sequence of linked CTFs* (*SLCTF*). Once the SLCTF is created, starting from the final CTF in the SLCTF, we successively back-propagate beliefs to the preceding CTFs via links between adjacent CTFs. To back-propagate beliefs from CTF_{k+1} to CTF_k , we choose a subset of links in L_k based on heuristics, which will be discussed later. Then, for each selected link (C, C', \tilde{C}) , we update the clique belief $\beta(C)$ as follows.

$$\beta(C) = \left(\frac{\beta(C)}{\sum_{C \setminus V_l} \beta(C)} \right) \sum_{\tilde{C} \setminus V_l} \beta(\tilde{C}) \quad (4)$$

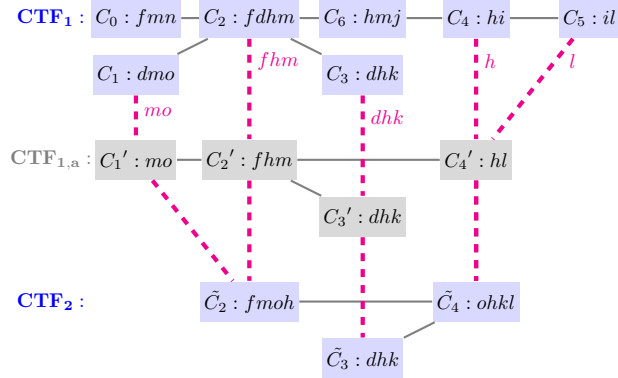


Figure 2: Links between corresponding cliques in CTF_1 , $CTF_{1,a}$ and CTF_2 for the example shown in Figure 1b. All links (C, C', \tilde{C}) are marked with dashed magenta lines and the link variables corresponding to each link are marked in magenta color.

This is followed by one round of message passing from C to all other cliques in the CT containing C . Once all CTFs are re-calibrated, we infer the marginal distribution of a variable using Equation 2 from the last CTF in which it is present.

For BNs, if incremental build is performed by adding variables in the topological order, then as shown in Theorem 2, the singleton marginals are consistent in CTFs $\{CTF_{k \geq I_E}\}$, where I_E is the index of the last CTF to which the factor corresponding to an evidence variable is added. Therefore, in this case, back-propagation of beliefs can be performed starting from CTF_{I_E} instead of starting from the last CTF. This reduces the effort required for belief update.

Heuristics for choice of links: To ensure that beliefs of all CTs in CTF_k are updated, at least one link must be chosen for each CT. It is also clear that for any CT in CTF_k more than one link may be required since variables that have low correlations in CTF_k could become tightly correlated when new factors are added in CTF_{k+1} . Empirically, we have found that updating via all links gives the best result. But it is expensive since each update via a link requires a round of message passing in CTF_k . Based on results over many benchmarks, we use the following heuristics to choose and schedule links for backward belief update.

(a) We first find the difference in the posterior marginals of all the link variables in both CTF_k and CTF_{k+1} . Link variables for which this difference is less than a threshold are discarded. For each remaining link variable, we find the clique C in CTF_k that contains the maximum number of link variables. The minimum set of cliques covering these remaining link variables is chosen for belief update.

(b) The updated beliefs depend on the order in which the links are used for update. Based on the difference in marginals, we form a priority queue with the cliques containing link variables that have the lowest change in marginals having the highest priority. This is to make sure that large belief updates do not get over-written by smaller ones. This could happen for example, if two variables, v_1 and v_2 , that are highly correlated in CTF_k become relatively uncorrelated in CTF_{k+1} due to the approximation. Assume that new factors added to CTF_{k+1} affect v_1 but not v_2 . A belief update via the link containing v_1 will make sure that its belief is consistent in CTF_k and CTF_{k+1} . Later, if we perform a belief update using a link containing v_2 , the previous larger belief update of v_1 will be overwritten by something smaller since the belief of v_2 is not very different in the two CTFs.

4 Results

All experiments were carried out on an Intel i9-12900 Linux system running Ubuntu 22.04.

Error metrics: For each non-evidence variable X_i , we measure error in terms of *Hellinger distance* between the exact marginal distribution $P(X_i)$ and the approximate marginal distribution $Q(X_i)$. It is computed as follows.

$$HD = \frac{1}{\sqrt{2}} \sqrt{\sum_{s \in \text{Domain}(X_i)} \{ \sqrt{P(X_i = s)} - \sqrt{Q(X_i = s)} \}^2} \quad (5)$$

We use two metrics namely, the *average Hellinger distance* (denoted as HD_{avg}) and the *maximum Hellinger distance* (denoted as HD_{max}) over all non-evidence variables in the network.

Benchmarks: We used the benchmark sets included in UAI repository [Ihler, 2006] and the Bayesian network repository [Scutari, 2007]. We classify instances for which exact solutions are present in the repository as ‘*small*’ and others as ‘*large*’.

Methods used for comparison: We compare the results obtained using our method with two existing variational methods namely, loopy belief propagation (LBP) [Murphy et al., 1999] and iterative join graph propagation (IJGP) [Mateescu et al., 2010], and an importance sampling based method called sample search [Gogate and Dechter, 2011]. IJGP is a mini-bucket based scheme where the maximum cluster size is bounded using a user-defined parameter and sample search uses an IJGP based proposal and cutset sampling (referred to as ‘ISSwc’ in this paper). Additional results showing a comparison with results published in Kelly et al. [2019] are included in the supplementary material.

Evaluation setup: The implementation of LBP was taken from LibDAI [Mooij, 2010, 2012]. For IJGP and ISSwc, we used implementations [Gogate, 2010, 2020] provided by the authors of these

methods. LBP, IJGP, ISSwc are implemented in C++. IBIA on the other hand has been implemented in Python3 and is thus, at a disadvantage in terms of runtime. We report results with runtime limits of 2 min and 20 min for small instances. In all cases, the memory limit was set to 8GB, which is the same as that used in UAI22 inference competition [UAI, 2022]. For IBIA, we set the maximum clique size bound mcs_p to 20 (referred to as ‘IBIA20’) when the time limit is 2 min and we set it to 23 (referred to as ‘IBIA23’) when the time limit is 20 min. mcs_{im} is empirically chosen as 5 less than mcs_p . The evaluation setup used for other methods is included in the supplementary material.

Table 1: Comparison of average HD_{avg} and average HD_{max} (shown in gray background) obtained using various inference methods with two runtime constraints, 2 min and 20 min. The minimum error obtained for each time limit is highlighted in bold. Entries are marked as ‘-’ where all instances could not be solved within the set time limit. The total number of instances solved by each method is shown in the last row. v_a : average number of variables, f_a : average number of factors, w_a : average induced width and dm_a : average of the maximum variable domain size.

| | Total #Inst | (v_a, f_a, w_a, dm_a) | 2 min | | | | 20 min | | | |
|-----------|-------------|-------------------------|--------------|-------------|--------------|--------------|--------|-------------|-------------|--------------|
| | | | LBP | IJGP | ISSwc | IBIA20 | LBP | IJGP | ISSwc | IBIA23 |
| BN | 97 | (637,637,28,10) | - | - | - | 2E-4 | 0.023 | - | - | 6E-5 |
| | | | - | - | - | 9E-3 | 0.230 | - | - | 2E-3 |
| GridBN | 29 | (595,595,37,2) | 0.075 | 0.011 | 0.003 | 5E-6 | 0.075 | 0.010 | 0.001 | 2E-7 |
| | | | 0.478 | 0.111 | 0.051 | 7E-4 | 0.478 | 0.094 | 0.015 | 1E-4 |
| Bnlearn | 26 | (256,256,7,16) | 0.010 | 0.011 | 0.012 | 7E-5 | 0.010 | 0.008 | 0.006 | 7E-6 |
| | | | 0.089 | 0.050 | 0.064 | 0.002 | 0.089 | 0.025 | 0.028 | 2E-4 |
| Pedigree | 24 | (853,853,24,5) | 0.075 | 0.035 | 0.033 | 0.009 | 0.075 | 0.033 | 0.021 | 0.008 |
| | | | 0.555 | 0.470 | 0.292 | 0.204 | 0.555 | 0.446 | 0.234 | 0.198 |
| Promedas | 64 | (618,618,21,2) | 0.032 | 0.124 | 0.030 | 0.013 | 0.032 | 0.120 | 0.021 | 0.010 |
| | | | 0.168 | 0.504 | 0.139 | 0.086 | 0.168 | 0.487 | 0.096 | 0.072 |
| DBN | 36 | (719,14205,29,2) | - | 0.081 | 0.016 | 0.020 | - | 0.060 | 2E-6 | 0.003 |
| | | | - | 0.919 | 0.766 | 0.261 | - | 0.879 | 2E-4 | 0.098 |
| ObjDetect | 79 | (60,210,6,16) | 0.022 | 0.004 | 0.018 | 0.002 | 0.022 | 3E-5 | 0.009 | 4E-4 |
| | | | 0.130 | 0.037 | 0.189 | 0.020 | 0.130 | 3E-4 | 0.061 | 0.006 |
| Grids | 8 | (250,728,22,2) | 0.433 | 0.247 | - | 0.088 | 0.433 | 0.123 | 0.056 | 0.002 |
| | | | 0.905 | 0.713 | - | 0.300 | 0.905 | 0.423 | 0.209 | 0.099 |
| CSP | 12 | (73,369,12,4) | 0.019 | 0.026 | - | 0.002 | 0.019 | 0.017 | 0.054 | 2E-4 |
| | | | 0.066 | 0.134 | - | 0.011 | 0.066 | 0.073 | 0.093 | 0.003 |
| Segment | 50 | (229,851,17,2) | 0.035 | 5E-6 | 5E-6 | 6E-5 | 0.035 | 5E-6 | 5E-6 | 1E-7 |
| | | | 0.258 | 7E-5 | 7E-5 | 0.001 | 0.258 | 7E-5 | 7E-5 | 4E-7 |
| Protein | 68 | (59,176,6,77) | 5E-4 | 0.003 | 0.003 | 6E-4 | 5E-4 | 0.007 | 0.001 | 3E-5 |
| | | | 0.007 | 0.094 | 0.049 | 0.039 | 0.007 | 0.230 | 0.015 | 0.002 |
| #Inst | 493 | | 481 | 487 | 485 | 493 | 485 | 491 | 487 | 493 |

Results: Table 1 has the results for the small benchmark sets. It reports the average of HD_{avg} and HD_{max} over all instances in each set. We compare results obtained using LBP, IJGP, IBIA20, IBIA23 and ISSwc for both time constraints. The minimum error obtained for each time limit is highlighted in bold. IBIA20 and IBIA23 solve all small instances within 2 min and 20 min respectively. In 2 min, the accuracy obtained with IBIA20 is either better than or comparable to the other solvers for all testcases except Segmentation and Protein. For Segmentation, IJGP and ISSwc give the least error and for Protein, LBP gives the least error. That said, for these instances, the errors obtained with IBIA20 are also small (average $HD_{avg} < 0.0006$ and average $HD_{max} < 0.04$). In 20 min, IBIA23 gives the least error in all testcases except DBN and ObjDetect. For DBNs, ISSwc reduces to exact inference in most instances and hence error obtained is close to zero. For ObjDetect, IJGP gives the least error closely followed by IBIA23. *Note that for many benchmarks the accuracy obtained with IBIA20 in 2 min is either better than or comparable to the accuracy obtained with other solvers in 20 min.*

A comparison of IBIA with results published in Kelly et al. [2019] for Gibbs sampling with Rao-blackwellisation (ARB) and IJGP is included in the supplementary material. It is seen that error obtained with IBIA is lower than both methods in majority of the testcases.

For BN instances, Table 2 compares the results obtained using IBIA20 when CTFs are constructed by adding factors in the topological order (columns marked as ‘TP’) with that obtained using a non-topological order (columns marked as ‘NTP’). We compare the maximum error in partition function (PR) and the average HD_{max} over all instances in each benchmark set. We observe that

Table 2: Comparison of maximum error in PR and average HD_{max} obtained using IBIA20 with CTFs constructed by adding factors in topological order (shown in columns marked ‘TP’) and that obtained using a non-topological order (shown in columns marked ‘NTP’). ev_a : Average number of evidence variables, $\Delta_{PR} = |\log_{10} PR - \log_{10} PR^*|$ where PR and PR^* are estimated and exact values.

| | #Inst | ev_a | Max Δ_{PR} | | Avg HD_{max} | |
|----------|-------|--------|-------------------|-------------|----------------|--------------|
| | | | NTP | TP | NTP | TP |
| Bnlearn | 26 | 0 | 0.02 | 0 | 0.023 | 0.002 |
| GridBN | 29 | 0 | 0.09 | 0 | 0.231 | 0.001 |
| Promedas | 64 | 7 | 1.5 | 0.4 | 0.322 | 0.086 |
| BN | 97 | 76 | 0.07 | 0.02 | 0.116 | 0.009 |
| Pedigree | 24 | 159 | 0.4 | 0.7 | 0.098 | 0.204 |

the topological ordering gives better accuracy for both PR and marginals in all testcases except Pedigree. GridBN and Bnlearn benchmarks have no evidence variables. Both runtime and memory complexity is better with topological ordering since marginals are consistent in all CTFs (using Corollary 2) and belief update is not needed. The average runtime with and without topological ordering was 1s and 146s respectively for GridBN instances and 0.3s and 1.3s for Bnlearn testcases.

To evaluate the scalability of the proposed algorithm, we ran it for large networks where the exact solutions are not known. Table 3 tabulates the percentage of large instances in each benchmark set that could be solved using IBIA within 2 min, 20 min and 60 min. For this experiment, we

Table 3: Percentage of large instances in each benchmark set solved by IBIA within 2, 20 and 60 minutes. v_a : average number of variables, f_a : average number of factors, w_a : average induced width and dm_a : average of the maximum domain-size.

| | Total #Inst | Average stats (v_a, f_a, w_a, dm_a) | Instances solved (%) | | |
|-----------|-------------|--|----------------------|--------|--------|
| | | | 2 min | 20 min | 60 min |
| BN | 22 | (1272,1272,51,17) | 64 | 100 | 100 |
| Promedas | 171 | (1207,1207,71,2) | 77 | 100 | 100 |
| ObjDetect | 37 | (60,1830,59,17) | 27 | 100 | 100 |
| Segment | 50 | (229,851,19,21) | 100 | 100 | 100 |
| Protein | 395 | (306,1192,21,81) | 75 | 97 | 98 |
| DBN | 78 | (944,47206,60,2) | 38 | 77 | 77 |
| Grids | 19 | (3432,10244,117,2) | 16 | 37 | 58 |
| CSP | 54 | (294,11725,175,41) | 31 | 54 | 59 |
| Type4b | 82 | (10822,10822,24,5) | 0 | 9 | 29 |

start with $mcs_p = 20$ and allow it to increase if incremental build results in a CTF with larger clique sizes. IBIA could solve all *large* instances in benchmark sets BN, Promedas, ObjDetect and Segmentation and most instances in Protein within 20 min. For other benchmarks, additional instances could be solved when the runtime was increased to 60 min. The memory required for the remaining Grids, DBN, CSP and Protein instances is more than 8 GB. The increased memory usage is due to the following reasons. Firstly, all calibrated CTFs in the SLCTF need to be stored in order to allow for back-propagation of beliefs and the memory required increases with the number of CTFs. The average number of CTFs in the remaining Grid, DBN and CSP benchmarks is 22, 58 and 80 respectively. Secondly, for benchmarks with large variable domain sizes, the number of variables present in each clique in a CTF is small. Therefore, approximation using exact and local marginalization becomes infeasible and the subsequent CTFs have clique sizes greater than mcs_p , which results in increased memory usage. This is seen in 9 out of 395 Protein instances and 12 out of 54 CSP instances. In addition to memory, the remaining Type4b instances also require additional runtime. This is because during belief update of each CTF, we perform one round of message passing for each selected link and the number of links is large in these instances.

5 Discussion

Limitations: While the belief update algorithm performs well for most benchmarks, it has some limitations. It is sequential and is performed link by link for each CTF that needs to be updated.

The time and space complexity depends on the number of CTFs in the sequence and the number of selected links, which is large in some testcases. Also, after belief-update of all CTFs is completed, beliefs of variables present in multiple CTFs need not be consistent. However, good accuracies are obtained when beliefs are inferred from the last CTF containing the variable. For BNs, we found that building CTFs in the topological order gives larger errors in some cases. A possible extension would be to have an efficient build strategy where the ordering is decided dynamically based on the properties of the graph structure.

Comparison with related work: Similar to other variational methods, accuracy of our method can be improved by increasing clique size bounds but this requires increase in both runtime and memory. However, the belief propagation step in the proposed technique is non-iterative and hence, does not have any convergence issues. Our method gives good accuracy since it performs belief based approximations. Other methods that use belief based approximations require expensive iterations of belief propagation for optimal selection of features or regions. Our approach also gives better accuracy than the state of art Gibbs sampling based method and comparable or better accuracies than sample search, with smaller runtimes.

References

- Shivani Bathla and Vinita Vasudevan. IBIA: An incremental build-infer-approximate framework for approximate inference of partition function. *arXiv preprint arXiv:2304.06366*, 2023.
- A. Choi, H. Chan, and A. Darwiche. On Bayesian network approximation by edge deletion. In *Uncertainty in Artificial Intelligence*, pages 128–135, 2005.
- Arthur Choi and Adnan Darwiche. An edge deletion semantics for belief propagation and its practical impact on approximation quality. In *National Conference on Artificial Intelligence and Innovative Applications of Artificial Intelligence Conference*, pages 1107–1114, 2006.
- Arthur Choi and Adnan Darwiche. Relax, compensate and then recover. In *JSAI International Symposium on Artificial Intelligence*, pages 167–180, 2010.
- M Julia Flores, José A Gámez, and Kristian G Olesen. Incremental compilation of Bayesian networks. In *Uncertainty in Artificial Intelligence*, pages 233–240, 2002.
- Brendan J Frey and David MacKay. A revolution: Belief propagation in graphs with cycles. In *Advances in Neural Information Processing Systems*, volume 10, 1998.
- Tal Friedman and Guy Van den Broeck. Approximate knowledge compilation by online collapsed importance sampling. *Advances in neural information processing systems*, 31, 2018.
- Alan E Gelfand. Gibbs sampling. *Journal of the American statistical Association*, 95(452):1300–1304, 2000.
- Vibhav Gogate. Iterative join graph propagation. <https://personal.utdallas.edu/~vibhav.gogate/ijgp.html>, 2010. Accessed: 2023-04-15.
- Vibhav Gogate. IJGP-sampling and samplesearch (PR and MAR tasks). <https://github.com/dechterlab/ijgp-samplesearch>, 2020. Accessed: 2023-01-15.
- Vibhav Gogate and Rina Dechter. Samplesearch: Importance sampling in presence of determinism. *Artificial Intelligence*, 175(2):694–729, 2011.
- Tom Heskes, Kees Albers, and Bert Kappen. Approximate inference and constrained optimization. In *Uncertainty in Artificial Intelligence*, pages 313–320, 2003.
- Alexander Ihler. UAI model files and solutions. <http://sli.ics.uci.edu/~ihler/uai-data/>, 2006. Accessed: 2021-10-15.
- Craig Kelly, Somdeb Sarkhel, and Deepak Venugopal. Adaptive Rao-Blackwellisation in Gibbs sampling for probabilistic graphical models. In *Artificial Intelligence and Statistics*, pages 2907–2915. PMLR, 2019.

- Steffen L Lauritzen and David J Spiegelhalter. Local computations with probabilities on graphical structures and their application to expert systems. *Journal of the Royal Statistical Society: Series B (Methodological)*, 50(2):157–194, 1988.
- Peng Lin, Martin Neil, and Norman Fenton. Improved high dimensional discrete Bayesian network inference using triplet region construction. *Journal of Artificial Intelligence Research*, 69:231–295, 2020.
- Qiang Liu and Alexander Ihler. Bounding the partition function using holder’s inequality. In *International Conference on Machine Learning*, pages 849–856, 2011.
- Robert Mateescu, Kalev Kask, Vibhav Gogate, and Rina Dechter. Join-graph propagation algorithms. *Journal of Artificial Intelligence Research*, 37:279–328, 2010.
- Joris M. Mooij. libDAI: A free and open source C++ library for discrete approximate inference in graphical models. *Journal of Machine Learning Research*, 11:2169–2173, August 2010.
- Joris M. Mooij. libDAI - A free/open source C++ library for discrete approximate inference. <https://github.com/dbtsai/libDAI/>, 2012. Accessed: 2021-10-15.
- Joris M. Mooij and Hilbert J. Kappen. Loop corrections for approximate inference on factor graphs. *Journal of Machine Learning Research*, 8(40):1113–1143, 2007.
- Kevin P. Murphy, Yair Weiss, and Michael I. Jordan. Loopy belief propagation for approximate inference: An empirical study. In *Uncertainty in Artificial Intelligence*, pages 467–475, 1999.
- Dan Roth. On the hardness of approximate reasoning. *Artificial Intelligence*, 82(1-2):273–302, 1996.
- Marco Scutari. Bayesian network repository. <https://www.bnlearn.com/bnrepository/>, 2007. Accessed: 2021-10-15.
- UAI. UAI 2022 - Competition. https://www.auai.org/uai2022/uai2022_competition, 2022.
- Martin J Wainwright, Tommi Jaakkola, and Alan Willsky. Tree-based reparameterization for approximate inference on loopy graphs. In T. Dietterich, S. Becker, and Z. Ghahramani, editors, *Advances in Neural Information Processing Systems*, volume 14, pages 1001–1008, 2002.
- Jonathan S Yedidia, William T Freeman, Yair Weiss, et al. Generalized belief propagation. In *Advances in Neural Information Processing Systems*, volume 13, pages 689–695, 2000.

A Results

A.1 Evaluation setup

For loopy belief propagation (LBP) [Murphy et al., 1999], we use the implementation provided in LibDAI [Mooij, 2010, 2012]. We set the tolerance limit to 10^{-3} when time limit is 2 min and 10^{-9} for 20 min. For iterative join graph propagation (IJGP) [Mateescu et al., 2010], we used the implementation available on the author’s webpage [Gogate, 2010]. The maximum cluster size in IJGP is set using the parameter *ibound*. This solver starts with the minimal value of *ibound* and increases it until the runtime and memory constraints are satisfied. A solution is obtained for each *ibound*. We report results obtained with the largest value of *ibound*. For sample search with IJGP-based proposal and cutset sampling (ISSwc) [Gogate and Dechter, 2011], we used the implementation provided by the authors on Github [Gogate, 2020]. For ISSwc, appropriate values of *ibound* and *w-cutset* bound are set by the tool based on the given runtime limit.

A.2 Additional results

For a fair comparison with IBIA using mcs_p of 20 (referred to as ‘IBIA20’), we also obtained the results for ISSwc after fixing both $ibound$ and $w-cutset$ bound to 20 (referred to as ‘ISSwc20’). Table 4 compares the average HD_{avg} and average HD_{max} over all instances in each benchmark set. We compare the results obtained using IBIA20, ISSwc20 and ISSwc with bounds determined by the solver (referred to as ‘ISSwcd’). The runtime limit was set to 2 min and 20 min, and the memory limit was set to 8 GB. The error obtained using IBIA20 is either smaller than or comparable to ISSwc20 and ISSwcd for both time limits in all testcases except DBN. For DBN, in 2 min, the average HD_{max} obtained with IBIA20 is significantly smaller than both variants of ISSwc, and the average HD_{avg} obtained with IBIA20 is comparable. However, in 20 min, both variants of ISSwc reduce to exact inference in many DBN instances and the average error obtained is close to zero. Since the errors obtained using ISSwcd are slightly lower than ISSwc20 in many benchmarks, we chose to compare with ISSwcd in the results presented in the main paper.

Table 5 compares the maximum Hellinger distance obtained using IBIA ($mcs_p=15,20$) with published results for adaptive Rao Blackwellisation (ARB) and iterative join graph propagation in Kelly et al. [2019]. The minimum error obtained is shown in bold. IBIA with $mcs_p = 20$ gives the least error in all cases. The error obtained with $mcs_p = 15$ is smaller than ARB and IJGP in all testcases except Grids_11, Grids_13 and Promedas_12.

Table 4: Comparison of average HD_{avg} and average HD_{max} (shown in gray background) obtained using IBIA with $mcs_p = 20$ (IBIA20), ISSwc with clique size bounds determined by the solver [Gogate, 2020] (ISSwcd) and ISSwc with $ibound$ and $w-cutset$ bound fixed to 20 (ISSwc20). Results are shown for two runtime limits, 2 min and 20 min. Entries are marked with ‘-’ if the solution for all testcases could not be obtained within the given time and memory limits. The minimum error obtained for a benchmark is highlighted in bold. The number of instances solved by each solver is shown in the last row. v_a : average number of variables, f_a : average number of factors, w_a : average induced width and dm_a : average of the maximum variable domain size.

| | Total #Inst | (v_a, f_a, w_a, dm_a) | 2 min | | | 20 min | |
|-----------|-------------|-------------------------|-------------|---------|--------------|--------------|--------------|
| | | | ISSwcd | ISSwc20 | IBIA20 | ISSwcd | ISSwc20 |
| BN | 97 | (637,637,28,10) | - | 0.037 | 2E-4 | - | 0.033 |
| | | | - | 0.145 | 9E-3 | - | 0.085 |
| GridBN | 29 | (595,595,37,2) | 0.003 | 0.005 | 5E-6 | 0.001 | 0.005 |
| | | | 0.051 | 0.065 | 7E-4 | 0.015 | 0.046 |
| Bnlearn | 26 | (256,256,7,16) | 0.012 | 0.036 | 7E-5 | 0.006 | 0.036 |
| | | | 0.064 | 0.094 | 0.002 | 0.028 | 0.093 |
| Pedigree | 24 | (853,853,24,5) | 0.033 | 0.028 | 0.009 | 0.021 | 0.021 |
| | | | 0.292 | 0.245 | 0.204 | 0.234 | 0.195 |
| Promedas | 64 | (618,618,21,2) | 0.030 | 0.042 | 0.013 | 0.021 | 0.033 |
| | | | 0.139 | 0.207 | 0.086 | 0.096 | 0.153 |
| DBN | 36 | (719,14205,29,2) | 0.016 | 0.011 | 0.020 | 2E-6 | 2E-6 |
| | | | 0.766 | 0.833 | 0.261 | 2E-4 | 2E-4 |
| ObjDetect | 79 | (60,210,6,16) | 0.018 | 0.039 | 0.002 | 0.009 | 0.004 |
| | | | 0.189 | 0.233 | 0.020 | 0.061 | 0.021 |
| Grids | 8 | (250,728,22,2) | - | - | 0.088 | 0.056 | - |
| | | | - | - | 0.300 | 0.209 | - |
| CSP | 12 | (73,369,12,4) | - | - | 0.002 | 0.054 | 0.069 |
| | | | - | - | 0.011 | 0.093 | 0.081 |
| Segment | 50 | (229,851,17,2) | 5E-6 | 0.002 | 6E-5 | 5E-6 | 5E-6 |
| | | | 7E-5 | 0.036 | 0.001 | 7E-5 | 7E-5 |
| Protein | 68 | (59,176,6,77) | 0.003 | 0.003 | 6E-4 | 0.001 | 0.001 |
| | | | 0.049 | 0.030 | 0.039 | 0.015 | 0.011 |
| #Inst | 493 | | 485 | 488 | 493 | 487 | 489 |

Table 5: Comparison of maximum Hellinger distance (HD_{max}) obtained using IBIA with published results for Gibbs sampling with adaptive Rao Blackwellisation (ARB) and iterative join graph propagation in Kelly et al. [2019]. Results obtained with $mcs_p = 15$ and $mcs_p = 20$ are shown in columns marked as IBIA15 and IBIA20 respectively. Runtimes (in seconds) for IBIA15 and IBIA20 are also shown. Estimates for ARB were obtained within 600 seconds⁺ [Kelly et al., 2019] and runtime for IJGP is not reported in Kelly et al. [2019]. The minimum error obtained for each benchmark is marked in bold. w : induced width, dm : maximum domain size

| | w | dm | HD_{max} | | | | Runtime (s) | |
|-------------|-----|------|----------------|-------|-------------|--------------|-------------|--------|
| | | | Merlin (IJGP)* | ARB* | IBIA15 | IBIA20 | IBIA15 | IBIA20 |
| Alchemy_11 | 19 | 2 | 0.777 | 0.062 | 0.004 | 1E-7 | 3.3 | 2.9 |
| CSP_11 | 16 | 4 | 0.513 | 0.274 | 0.100 | 0.034 | 0.5 | 3.4 |
| CSP_12 | 11 | 4 | 0.515 | 0.275 | 0.028 | 6E-7 | 0.1 | 0.1 |
| CSP_13 | 19 | 4 | 0.503 | 0.290 | 0.085 | 0.051 | 0.9 | 2.9 |
| Grids_11 | 21 | 2 | 0.543 | 0.420 | 0.590 | 0.166 | 1.1 | 3.5 |
| Grids_12 | 12 | 2 | 0.645 | 0.432 | 3E-7 | 3E-7 | 0.0 | 0.0 |
| Grids_13 | 21 | 2 | 0.500 | 0.544 | 0.962 | 0.246 | 1.1 | 3.6 |
| Pedigree_11 | 19 | 3 | 0.532 | 0.576 | 0.016 | 5E-7 | 0.5 | 0.1 |
| Pedigree_12 | 19 | 3 | 0.562 | 0.506 | 0.023 | 4E-7 | 0.3 | 0.1 |
| Pedigree_13 | 19 | 3 | 0.577 | 0.611 | 5E-7 | 5E-7 | 0.1 | 0.1 |
| Promedus_11 | 18 | 2 | 1.000 | 0.373 | 0.049 | 5E-7 | 1.4 | 0.5 |
| Promedus_12 | 20 | 2 | 1.000 | 0.358 | 0.657 | 0.242 | 2.8 | 4.1 |
| Promedus_13 | 10 | 2 | 1.000 | 0.432 | 5E-7 | 5E-7 | 0.4 | 0.4 |

* The results tabulated in Kelly et al. [2019] report $-\log_2 HD_{max}$. The table above has the corresponding values of HD_{max} .

⁺ Published results for ARB were obtained on a system running Ubuntu 18.04, with 16GB of RAM, 6 CPUs and 2 hardware threads per CPU [Kelly et al., 2019].

B Pseudo-code

Algorithm 1 shows the steps in the proposed algorithm for the inference of marginals. We first convert the PGM into a sequence of linked CTFs ($SLCTF$) that contains a sequence of calibrated CTFs ($SCTF = \{CTF_k\}$) and a list of links between adjacent CTFs ($SL = \{L_k\}$). Functions *BuildCTF* and *ApproximateCTF* are used for incremental construction of CTFs and approximation of CTFs respectively. The steps in these functions are explained in detail in Algorithms 1 and 2 in Bathla and Vasudevan [2023]. Links between adjacent CTFs are found using the function *FindLinks* and belief update in the SLCTF is performed using the function *BeliefUpdate*. Following this, the marginal of a variable v is inferred from clique beliefs in the last CTF that contains v (line 23).

C Proofs

Notations

| | |
|--------------|---|
| Φ_k | Set of factors added during construction of CTF_k |
| X_k | Set of all variables in CTF_k |
| $X_{k,a}$ | Set of all variables in $CTF_{k,a}$ |
| Pa_y | Set of parents of variable y in the BN |
| Y_k | Set of new variables added during construction of CTF_k |
| e_k | Evidence state corresponding to all evidence variables in Y_k |
| Pa_{Y_k} | Parents of variables in Y_k in the BN |
| C | A clique in CTF_k |
| C' | A clique in $CTF_{k,a}$ |
| SP | Sepset associated with an edge in CTF_k |
| SP' | Sepset associated with an edge in $CTF_{k,a}$ |
| Z_k | Normalization constant of the distribution encoded by calibrated beliefs in CTF_k |
| $Q(X_k)$ | Probability distribution corresponding to CTF_k |
| $Q(X_{k,a})$ | Probability distribution corresponding to $CTF_{k,a}$ |

Propositions related to inference of marginals: Let CTF_k be a CTF in the SCTF generated by the IBIA framework and $CTF_{k,a}$ be the corresponding approximate CTF.

Proposition 5. *The joint belief of variables contained within any clique in the approximate CTF $CTF_{k,a}$ is the same as that in CTF_k .*

Proof. The approximation algorithm has two steps, exact marginalization and local marginalization.

Let ST_v be the subtree of $CTF_{k,a}$ that has all the cliques containing a non-interface variable v . During exact marginalization, a new clique C_c is obtained after collapsing cliques in ST_v and removing v . The clique belief for C_c is obtained after marginalizing the joint probability distribution of ST_v over all states in the domain of variable v , as follows.

$$\beta(C_c) = \sum_{D_v} \left(\frac{\prod_{C_i \in ST_v} \beta(C_i)}{\prod_{SP \in ST_v} \mu(SP)} \right)$$

where SP denotes sepsets in ST_v and D_v denotes the domain of variable v . Summing over the states of v does not change the joint beliefs of the remaining variables in C_c .

During local marginalization, a new clique C'_i is obtained after removing a variable v from an existing clique C_i . The clique belief $\beta(C'_i)$ is obtained after summing the clique belief $\beta(C_i)$ over the states of variable v as shown below.

$$\beta(C'_i) = \sum_{D_v} \beta(C_i)$$

Once again, summing over the states of v does not alter the joint belief of the remaining variables in C'_i . \square

Proposition 6. *The clique beliefs in CTF_k account for all factors added to $\{CTF_1, \dots, CTF_k\}$.*

Proof. CTF_1 is constructed by adding factors to an initial CTF that contains a set of disjoint cliques corresponding to a subset of factors with disjoint scopes. Let Φ_1 be the set of all factors present in CTF_1 . After calibration, the belief of cliques in CTF_1 can be computed as follows.

$$\beta(C) = \sum_{X_1 \setminus C} \frac{\prod_{C \in CTF_1} \beta(C)}{\prod_{SP \in CTF_1} \mu(SP)} = \sum_{X_1 \setminus C} \prod_{\phi \in \Phi_1} \phi, \quad C \in CTF_1$$

Therefore, clique beliefs in CTF_1 account for all factors in Φ_1 . $CTF_{1,a}$ is obtained after approximating CTF_1 . Using Proposition 5, the clique and sepset beliefs in $CTF_{1,a}$ is the same as in CTF_1 that is,

$$\beta(C') = \sum_{X_1 \setminus C'} \frac{\prod_{C \in CTF_1} \beta(C)}{\prod_{SP \in CTF_1} \mu(SP)} = \sum_{X_1 \setminus C'} \prod_{\phi \in \Phi_1} \phi, \quad C' \in CTF_{1,a} \quad (6)$$

$$\mu(SP') = \sum_{X_1 \setminus SP'} \frac{\prod_{C \in CTF_1} \beta(C)}{\prod_{SP \in CTF_1} \mu(SP)} = \sum_{X_1 \setminus SP'} \prod_{\phi \in \Phi_1} \phi, \quad SP' \in CTF_{1,a} \quad (7)$$

CTF_2 is constructed by adding factors in Φ_2 to $CTF_{1,a}$. Therefore, after calibration, beliefs of cliques in CTF_2 can be computed as follows.

$$\beta(C) = \sum_{X_2 \setminus C} \frac{\prod_{C' \in CTF_{1,a}} \beta(C')}{\prod_{SP' \in CTF_{1,a}} \mu(SP')} \prod_{\phi \in \Phi_2} \phi, \quad C \in CTF_2 \quad (8)$$

Using Equations 6 and 7, the beliefs of all cliques and sepsets in $CTF_{1,a}$ account for all factors in Φ_1 . Therefore, as seen from equation 8, the overall distribution corresponding to CTF_2 corresponds to all factors in Φ_1 and Φ_2 .

A similar procedure can be repeated for subsequent CTFs to show that the proposition holds true for all CTFs in the sequence. \square

Propositions related inference in BNs:

BNs are directed probabilistic graphical models where the graph induced by the set of factors is a directed acyclic graph (DAG). *Parents* of a variable y in the BN are nodes that are connected via incoming edges to y . Each factor in a BN is the conditional probability distribution (CPD) of a variable given the states of its parents. The following propositions are related to inference in BNs assuming that each CTF in the SCTF is constructed by adding factors in the topological order. By this, we mean that the factor corresponding to the variable y is added only after the factors corresponding to all parent variables in Pa_y have been added to some CTF in the sequence.

Let \mathcal{Y} be the list of all variables in the BN, arranged in topological order. The first set of variables in this list are the variables that do not have any parents and the initial CTF, CTF_0 , is obtained as disjoint cliques containing these variables. Following this, the CPDs corresponding to the remaining variables in \mathcal{Y} are added to construct all CTFs in the sequence. Let Y_k denote the set of variables whose CPDs are added during construction of CTF_k , e_k denote the evidence states of all evidence variables in Y_k and Pa_{Y_k} denote the parents of variables in Y_k in the BN.

Proposition 7. *The product of factors added in CTFs, $\{CTF_1, \dots, CTF_k\}$ is a valid probability distribution whose normalization constant is the probability of evidence states e_1, \dots, e_k .*

Proof. For each variable $y \in \{Y_1, \dots, Y_k\}$, the corresponding CPD $P(y|Pa_y)$ is added to some CTF in $\{CTF_1, \dots, CTF_k\}$. CPDs corresponding to parents of y are always added before CPD of y is added. Therefore, the product of all CPDs added up to CTF_k is a valid probability distribution whose normalization constant (NC) is the probability of evidence states e_1, \dots, e_k .

$$\prod_{i=1, \dots, k} \prod_{y \in Y_i} P(y|Pa_y) = P(Y_1, \dots, Y_k, e_1, \dots, e_k)$$

□

Proposition 8. *The normalization constant of the distribution encoded by the calibrated beliefs in CTF_k is the estimate of probability of evidence states e_1, \dots, e_k .*

Proof. The initial factors assigned to CTF_1 are CPDs of variables in Y_1 . Therefore, using Proposition 7, the NC obtained after calibration is $Z_1 = P(e_1)$.

$CTF_{1,a}$ is obtained after approximation of CTF_1 . All CTs in $CTF_{1,a}$ are calibrated CTs (refer Proposition 5 in Bathla and Vasudevan [2023]). Since the approximation algorithm ensures that connected CTs remain connected, each CT in CTF_1 corresponds to a single CT in $CTF_{1,a}$. Using Proposition 5, we know that the belief of variables within any clique in $CTF_{1,a}$ is same as that in CTF_1 . Therefore, the normalization constant (NC) of the clique beliefs in corresponding CTs in CTF_1 and $CTF_{1,a}$ is also the same. Therefore, the overall NC of $CTF_{1,a}$ which is the product of NCs of disjoint CTs is also the same in both CTFs. However, due to local marginalization, the overall distribution represented by $CTF_{1,a}$ is approximate. The probability distribution corresponding to $CTF_{1,a}$ can be written as follows.

$$\begin{aligned} Q(X_{1,a}|e_1) &= \frac{1}{Z_1} \frac{\prod_{C' \in CTF_{1,a}} \beta(C')}{\prod_{SP' \in CTF_{k,a}} \mu(SP')} \\ \implies Z_1 Q(X_{1,a}|e_1) &= Q(X_{1,a}, e_1) \end{aligned} \quad (9)$$

where $X_{1,a}$ is the set of variables in $CTF_{1,a}$.

CTF_2 is obtained after adding a new set of CPDs of variables in Y_2 to $CTF_{1,a}$. Let $X_2 = X_{1,a} \cup Y_2$ denote the set of all variables in CTF_2 . The NC of the distribution encoded by CTF_2 (Z_2) can be computed as follows.

$$\begin{aligned} Z_2 &= \sum_{X_2} \frac{\prod_{C' \in CTF_{1,a}} \beta(C')}{\prod_{SP' \in CTF_{1,a}} \mu(SP')} \prod_{y \in Y_2} P(y|Pa_y) \\ &= \sum_{X_2} Q(X_{1,a}, e_1) P(Y_2, e_2 | Pa_{Y_2}) \quad (\text{using Equation 9}) \end{aligned} \quad (10)$$

where e_2 are evidence states in Y_2 . Since variables in $X_{1,a} \subseteq Y_1$ are non-descendants of Y_2 , the following holds true.

$$P(Y_2, e_2 \mid X_{1,a}, Pa_{Y_2}) = P(Y_2, e_2 \mid Pa_{Y_2}) \quad (11)$$

Using Equations 10 and 11, it follows that

$$\begin{aligned} Z_2 &= \sum_{X_2} Q(X_{1,a}, e_1) P(Y_2, e_2 \mid X_{1,a}, Pa_{Y_2}) \\ &= \sum_{X_2} Q(X_2, e_1, e_2) \quad (\because Pa_{Y_2} \subseteq X_2 = Y_2 \cup X_{1,a}) \\ &= Q(e_1, e_2) \end{aligned}$$

A similar procedure can be repeated for subsequent CTFs to show that the property holds true for all CTFs in the sequence. \square

Theorem 2. *Let I_E denote the index of the last CTF in the sequence where the factor corresponding to an evidence variable is added. The posterior marginals of variables present in CTFs $\{CTF_k, k \geq I_E\}$ are preserved and can be computed from any of these CTFs.*

Proof. Let v be a variable present in $C_v \in CTF_{I_E}$, $C'_v \in CTF_{I_E,a}$ and $\tilde{C}_v \in CTF_{I_E+1}$. From Proposition 5, the belief of variable v in C'_v is same as that in C_v . Therefore,

$$\sum_{X_{I_E,a} \setminus v} \frac{\prod_{C' \in CTF_{I_E,a}} \beta(C')}{\prod_{SP' \in CTF_{I_E,a}} \mu(SP')} = \sum_{C'_v \setminus v} \beta(C'_v) = \sum_{C_v \setminus v} \beta(C_v) \quad (12)$$

CTF_{I_E+1} is constructed by adding CPDs of variables in Y_{I_E+1} to $CTF_{I_E,a}$. Therefore, after calibration, clique belief $\tilde{C}_v \in CTF_{I_E+1}$ can be computed as follows,

$$\beta(\tilde{C}_v) = \sum_{X_{I_E+1} \setminus \tilde{C}_v} \frac{\prod_{C' \in CTF_{I_E,a}} \beta(C')}{\prod_{SP' \in CTF_{I_E,a}} \mu(SP')} P(Y_{I_E+1} \mid Pa_{Y_{I_E+1}}) \quad (\because e_{I_E+1} = \emptyset)$$

The belief of variable v can be computed from clique belief of \tilde{C}_v as shown below.

$$\begin{aligned} \sum_{\tilde{C}_v \setminus v} \beta(\tilde{C}_v) &= \sum_{\tilde{C}_v \setminus v} \sum_{X_{I_E+1} \setminus \tilde{C}_v} \frac{\prod_{C' \in CTF_{I_E,a}} \beta(C')}{\prod_{SP' \in CTF_{I_E,a}} \mu(SP')} P(Y_{I_E+1} \mid Pa_{Y_{I_E+1}}) \\ &= \sum_{X_{I_E+1} \setminus v} \frac{\prod_{C' \in CTF_{I_E,a}} \beta(C')}{\prod_{SP' \in CTF_{I_E,a}} \mu(SP')} P(Y_{I_E+1} \mid Pa_{Y_{I_E+1}}) \end{aligned}$$

Since the set of new variables $Y_{I_E+1} = X_{I_E+1} \setminus X_{I_E,a}$, the above equation be re-written as follows.

$$\begin{aligned} \sum_{\tilde{C}_v \setminus v} \beta(\tilde{C}_v) &= \sum_{X_{I_E,a} \setminus v} \frac{\prod_{C' \in CTF_{I_E,a}} \beta(C')}{\prod_{SP' \in CTF_{I_E,a}} \mu(SP')} \sum_{Y_{I_E+1}} P(Y_{I_E+1} \mid Pa_{Y_{I_E+1}}) \\ &= \sum_{X_{I_E,a} \setminus v} \frac{\prod_{C' \in CTF_{I_E,a}} \beta(C')}{\prod_{SP' \in CTF_{I_E,a}} \mu(SP')} \quad (\because \sum_{Y_{I_E+1}} P(Y_{I_E+1} \mid Pa_{Y_{I_E+1}}) = 1) \\ &= \sum_{C_v \setminus v} \beta(C_v) \quad (\text{using Equation 12}) \end{aligned} \quad (13)$$

Summing over the states of v , we get

$$\sum_{\tilde{C}_v} \beta(\tilde{C}_v) = \sum_{C_v} \beta(C_v) \quad (14)$$

Using Equations 13 and 14, the posterior marginal inferred from clique $\tilde{C}_v \in CTF_{I_E+1}$ is same as that inferred from clique $C_v \in CTF_{I_E}$.

The above procedure can be repeated to show that the posterior marginal of v is also consistent in all subsequent CTFs that contain v . \square

Algorithm 1 InferMarginals (Φ, mcs_p, mcs_{im})

Input: Φ : Set of factors in the PGM
 mcs_p : Maximum clique size bound for each CTF in the sequence
 mcs_{im} : Maximum clique size bound for the approximate CTF
Output: MAR : Map containing marginals $\langle variable : margProb \rangle$

- 1: Initialize: $MAR = \langle \rangle$ \triangleright Map $\langle variable : margProb \rangle$
 $S_v = \cup_{\phi \in \Phi} Scope(\phi)$ \triangleright Set of all variables in the PGM
 $SCTF = []$ \triangleright Sequence of calibrated CTFs
 $SL = []$ \triangleright List of list of links between all adjacent CTFs
 $k = 1$ \triangleright Index of CTF in $SCTF$
- 2: **while** $\Phi.isNotEmpty()$ **do** \triangleright Convert PGM Φ to $SLCTF = \{SCTF, SL\}$
- 3: **if** $k == 1$ **then**
- 4: $CTF_0 \leftarrow$ Disjoint cliques corresponding to factors in Φ with disjoint scopes
- 5: \triangleright Add factors to CTF_0 using BuildCTF (Algorithm 1 in Bathla and Vasudevan [2023])
- 6: $CTF_1, \Phi_1 \leftarrow$ BuildCTF (CTF_0, Φ, mcs_p) $\triangleright \Phi_1$: Subset of factors in Φ added to CTF_1
- 7: $\Phi \leftarrow \Phi \setminus \Phi_1$ \triangleright Remove factors added to CTF_1 from Φ
- 8: **else**
- 9: \triangleright Add factors to $CTF_{k-1,a}$ using BuildCTF (Algorithm 1 in Bathla and Vasudevan [2023])
- 10: $CTF_k, \Phi_k \leftarrow$ BuildCTF ($CTF_{k-1,a}, \Phi, mcs_p$) $\triangleright \Phi_k$: Subset of factors in Φ added to CTF_k
- 11: $\Phi \leftarrow \Phi \setminus \Phi_k$ \triangleright Remove factors added to CTF_k from Φ
- 12: $L_{k-1} \leftarrow$ FindLinks($CTF_{k-1}, CTf_{k-1,a}, CTF_k$) $\triangleright L_{k-1}$: List of links between CTF_{k-1}, CTF_k
- 13: $SL.append(L_{k-1})$ \triangleright Add L_{k-1} to the sequence of links SL
- 14: **end if**
- 15: Calibrate CTF_k using belief propagation
- 16: $SCTF.append(CTF_k)$ \triangleright Add CTF_k to the sequence $SCTF$
- 17: \triangleright Reduce clique sizes to mcs_{im} using ApproximateCTF (Algorithm 2 in Bathla and Vasudevan [2023])
- 18: $CTF_{k,a} \leftarrow$ ApproximateCTF (CTF_k, Φ, mcs_{im})
- 19: $k \leftarrow k + 1$
- 20: **end while**
- 21: $SLCTF = \{SCTF, SL\}$ \triangleright Sequence of linked CTFs
- 22: BeliefUpdate($SLCTF$) \triangleright Re-calibrate CTFs so that beliefs in all CTFs account for all factors
- 23: $MAR[v] \leftarrow$ Find marginal of v from CTF_j s.t. $v \in CTF_k, v \notin CTF_{k+1} \quad \forall v \in S_v$ \triangleright Infer marginals
- 24:
- 25: **procedure** FINDLINKS($CTF_{k-1}, CTf_{k-1,a}, CTF_k$)
- 26: \triangleright Each link is a triplet consisting of $C \in CTF_{k-1}, C' \in CTf_{k-1,a}$ and $\tilde{C} \in CTF_k$
- 27: **for** $C' \in CTf_{k-1,a}$ **do** \triangleright Find links corresponding to each clique C' in $CTf_{k-1,a}$
- 28: \triangleright Find list of corresponding cliques in CTF_{k-1}, L_c
- 29: **if** $C'.isCollapsedClique$ **then** $\triangleright C'$ is obtained after exact marginalization
- 30: $L_c \leftarrow$ List of cliques in CTF_{k-1} that were collapsed to form C'
- 31: **else** $\triangleright C'$ is either obtained after local marginalization or it is present as is in CTF_k
- 32: $C \leftarrow$ Clique in CTF_{k-1} s.t. $C' \subseteq C; L_c = [C]$
- 33: **end if**
- 34: Find clique \tilde{C} in CTF_k s.t. $C' \subseteq \tilde{C}$
- 35: \triangleright Add all links corresponding to C'
- 36: **for** $C \in L_c$ **do** $L_{k-1}.append((C, C', \tilde{C}))$ **end for**
- 37: **end for**
- 38: **return** L_{k-1}
- 39: **end procedure**
- 40:
- 41: **procedure** BELIEFUPDATE($SLCTF$)
- 42: $SCTF, SL = SLCTF$
- 43: **for** $k \in len(SCTF)$ **down to** 2 **do** \triangleright Update beliefs in $\{CTF_k, k < len(SCTF)\}$
- 44: $CTF_{k-1} \leftarrow SCTF[k-1]; CTF_k = SCTF[k]; L_{k-1} = SL[k-1]$
- 45: $L_s \leftarrow$ Choose a subset of links in L_{k-1} using heuristics described in Section 3.2
- 46: **for** $(C, C', \tilde{C}) \in L_s$ **do** \triangleright Back-propagate beliefs from CTF_k to CTF_{k-1} via all selected links
- 47:
$$\beta(C) = \frac{\beta(C)}{\sum_{C' \in \{C \cap C'\}} \beta(C')} \sum_{\tilde{C} \in \{C \cap \tilde{C}'\}} \beta(\tilde{C})$$
 \triangleright Update $\beta(C) \in CTF_{k-1}$ based on $\beta(\tilde{C}) \in CTF_k$
- 48: Update belief of all other cliques in CTF_{k-1} using single pass message passing with C as root
- 49: **end for**
- 50: **end for**
- 51: **end procedure**
